

Photopolymerized microscopic vortex beam generators: Precise delivery of optical orbital angular momentum

Etienne Brasselet,^{1,a)} Mangirdas Malinauskas,² Albertas Žukauskas,² and Saulius Juodkazis³

¹*Centre de Physique Moléculaire Optique et Hertzienne, Université Bordeaux I, CNRS, 351 Cours de la Libération, 33405 Talence Cedex, France*

²*Department of Quantum Electronics, Laser Nanophotonics Group, Physics Faculty, Vilnius University, Saulėtekio 9, LT-10222 Vilnius, Lithuania*

³*Centre for Micro-Photonics, Faculty of Engineering and Industrial Sciences, Swinburne University of Technology, Hawthorn, VIC 3122, Australia*

(Received 22 September 2010; accepted 25 October 2010; published online 23 November 2010)

Direct femtosecond laser photopolymerization is used to fabricate high resolution microscopic spiral phase plates. The total phase change all around their center is prepared to be a integer multiple of 2π for the operating wavelength in the visible domain. The optical performances of the spiral plates are measured and we propose a simple single beam interferometric technique to characterize the phase singularity of the generated vortex beams. The experimental results are compared to simulations and a satisfying agreement is obtained. Potential of large scale fabrication, templating, and smart spiral plate architectures are also illustrated. © 2010 American Institute of Physics. [doi:10.1063/1.3517519]

Direct laser writing technique using femtosecond laser pulses has been revealed versatile and useful for the high precision material removal, modification, or deposition. Indeed, if standard approaches can routinely deal with $\lambda/2$ resolution, one or two-color supersolution techniques have recently been proposed to reach $\lambda/20$ resolution.^{1,2} Despite inherent serial processing limitations, the availability of high-repetition femtosecond-lasers and precise fast scanning stages and galvano-mirrors allow for an increasing number of applications. The latter includes prototyping of micro-optical and plasmonic elements, dicing, drilling, edge-isolation in solar cells, direct print of electronic circuitry by light-induced forward transfer, and bioscaffolds.^{3–6} The fabrication time is another issue of paramount importance. In particular a two-step approach can be used to reduce the fabrication time of micro-optical elements by two orders of magnitude compared to straightforward bulk laser photopolymerization. It consists in defining a three-dimensional shell inside the bulk of a negative photoresist and, after development, exposing the entire microstructure to uv light in order to provide a uniform cross-linking inside the shell, which corresponds to the bulk of the desired optical element.⁷ Indeed such an approach was recently used to produce dense arrays of microlenses.⁸

We propose to use direct laser writing to fabricate photopolymerized optical vortex beam generator architectures at the micron scale. Vortex beams refer to light field endowed with on-axis phase singularity, which corresponds to a local azimuthal phase dependence of the electric field of the form $\exp(i\ell\phi)$ where ℓ is called the topological charge and ϕ is the azimuthal angle. Such beams carry nonzero orbital angular momentum⁹ and have many applications (e.g., see Ref. 10 for a review). Among all possible techniques to generate vortex beams, the use of so-called spiral phase plates (SPPs), whose complex transmittance has a linear phase dependence

with respect to ϕ , has started in 1992.¹¹ Since then, SPPs have been revealed useful over a broad range of electromagnetic radiation wavelength, from millimeter waves¹² to x rays.¹³ However, most of the realizations correspond to macroscopic SPPs made by micromachining followed by molding techniques, electron beam lithography, or laser writing followed by plasma etching. Recently, the first realization using a standalone direct laser writing technique allowed for drastic downsizing of SPPs¹⁴ thus enabling *in situ* control of the orbital angular momentum delivered by optical tweezers. Although the latter concept has been illustrated by the observation of a light-driven rotation of an optically trapped micron-size optical element,¹⁴ the direct characterization of the optical vortex beams obtained from microscopic SPPs have however not been reported so far.

Here we show fast and reliable femtosecond-fabrication of high precision SPPs whose height is defined as $h=h_0+h_1\frac{\phi}{2\pi}$ with h_0 the base height of the structure, h_1 the step height, and ϕ the azimuthal angle around the spiral axis. The step height control reaches ~ 10 nm fidelity for both small (few microns) and large (of the order of 100 μm) microstructures and a smooth phase ramp is obtained. The generation of vortex beams is experimentally demonstrated by direct analysis of the output spatial distribution of both intensity and phase for an incident fundamental Gaussian beam. In particular, we present a simple single beam original interferometric technique to characterize the phase singularity of the generated vortex beams. The observations are then compared to simulations and a satisfying agreement is obtained.

The employed femtosecond-laser polymerization procedures are optimized for resist response [we used resist SZ2080¹⁵], high spatial precision, and short fabrication time by using a fast shell-definition with postexposure, as reported elsewhere.^{7,16} We used 150 or 80 fs duration laser pulses with central wavelength $\lambda=800$ nm tightly focused with an objective lens of numerical aperture $\text{NA}=1.4$ and scanned

^{a)}Electronic mail: e.brasselet@cpmoh.u-bordeaux1.fr.

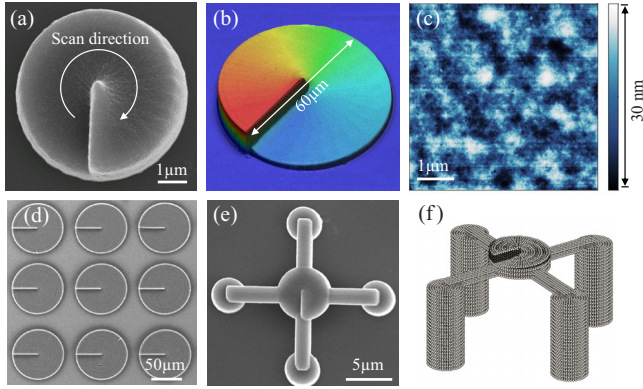


FIG. 1. (Color online) (a) SEM images of a 5 μm diameter SPP, the arrow indicates the laser writing scan direction. (b) Optical profilometry image of a 60 μm diameter SPP with $\ell=5$ for an operating wavelength in air $\lambda'=633$ nm. (c) Atomic force microscope image of the SPP surface. (d) and (e) Top-view SEM image of an array of SPPs and a single SPP suspended in the air, respectively. (f) Three-dimensional view of the structure shown in panel (e) where each point refers to the location of a laser written voxel.

inside a drop-cast resist to define the SPP. The sample was translated in 10 nm steps at 50 $\mu\text{m}/\text{s}$ scanning speed at intensities of $\sim 0.1\text{--}0.2$ TW/cm² per pulse to ensure efficient radical generation and controlled polymerization.¹⁶ In all cases, the writing spot is scanned concentrically with fixed 160 nm scan-arc steps with 75% radial overlap between neighbor lines, which ensure identical exposure conditions from the center to the outer part of the SPP. In addition, flat surface is naturally improved by diffusion-propagation of polymerization and self-smoothing caused by surface effects.^{8,17} The fabrication process lasted ~ 20 min when the SPP surface is defined first. The rest of the volume is then exposed at 5 cm distance from a 2×4 W two-wavelength uv lamp (254 and 366 nm) for ~ 15 min after the development of resist, but keeping the sample immersed in a fresh rinsing solvent. This is required for the exact definition of the SPP's step height $h_1 = \ell\lambda'/(n' - n_0)$ with an accuracy better than $\lambda/15$. We choose integer topological charges ℓ and SPPs are designed to operate at $\lambda'=633$ nm for which $n'=1.504$ is the refractive index of the sol-gel films measured from a m -line prism coupling experiment¹⁸ and $n_0=1$ is the refractive index of medium surrounding the SPP (here air).

Typical scanning electron microscopy (SEM) images of small and large polymerized SPPs are shown in Figs. 1(a) and 1(d), which also illustrates the possibility to fabricate two-dimensional arrays of SPPs on a planar substrate. In fact, more complex three-dimensional microscopic architectures endowed with vortex beam generation capabilities can also be realized. An example is given in Figs. 1(e) and 1(f) where a SPP suspended a few microns above the substrate is shown. The polymerized structures have also been analyzed by optical profilometry, see Fig. 1(b), and atomic force microscope imaging, see Fig. 1(c). The surface roughness is found to be better than $\lambda/20$ for visible wavelength, which is adequate for demanding applications in wavefront shaping at the micron scale.

Then, the optical performances of the fabricated vortex generators are evaluated using on-axis Gaussian laser beam illumination at 633 nm wavelength and normal incidence. For this purpose we define w_0 as the Gaussian beam waist at $\exp(-2)$ of its maximal intensity and R is the SPP radius. The

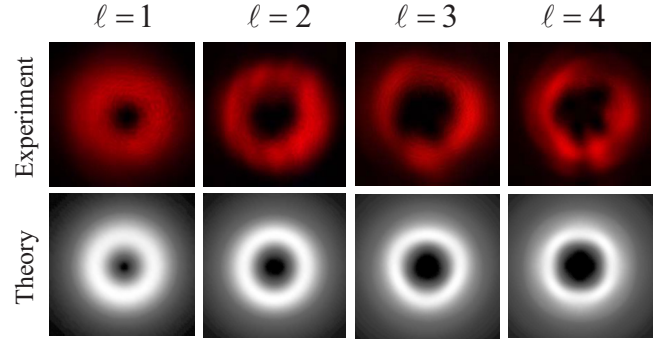


FIG. 2. (Color online) Far field intensity pattern when a focused Gaussian beam (waist w_0) is normally incident onto a SPP (radius R) located in the focal plane of the incident beam with different integer topological charges ℓ . The data correspond to $w_0/R=1/2$ with $R=40$ μm and the distance between the SPP plane and the observation plane is a few tens of the Rayleigh distance. Upper row: experimental data. Bottom row: calculated profiles.

observed far field intensity patterns obtained from SPPs with $R=40$ μm radius and integer topological charge $\ell=(1,2,3,4)$ are shown in Fig. 2 (upper row) in the case $w_0/R=1/2$. In practice, the distance z between the SPP plane and the observation plane is a few tens of the Rayleigh distance $z_0 = \pi w_0^2/\lambda'$. In agreement with main features of vortex beams¹⁹ we observe a doughnut intensity pattern whatever ℓ with a vortex core region that increases with ℓ . The comparison with the expected intensity pattern in the observation plane associated to the cylindrical coordinate system (ρ, θ, z) is carried out by considering the diffraction of a Gaussian beam by the SPP. By considering that the focal plane of the incident focused Gaussian beam is located at $z=0$ the Fresnel diffraction in the paraxial approximation gives, up to an unimportant rotation around the z axis

$$I(\rho, \theta, z) \propto \left| e^{i\ell\theta} \int_0^R \mathcal{J}_\ell(\rho, r, z) r dr + \int_R^\infty \mathcal{J}_0(\rho, r, z) r dr \right|^2, \quad (1)$$

where

$$\mathcal{J}_\ell(\rho, r, z) = \exp\left(i \frac{k' r^2}{2z} - \frac{r^2}{w_0^2}\right) J_\ell\left(\frac{k' \rho r}{z}\right) \quad (2)$$

with $k'=2\pi/\lambda'$ the wavevector in free space and J_n the n th order Bessel function of the first kind. The calculated profiles are shown in the bottom row of Fig. 2 and exhibit a satisfying agreement with the observations. Nevertheless, the expected rotational symmetry is slightly broken for larger values of ℓ , see for instance $\ell=4$ in the upper row of Fig. 2. This is explained by imperfectly matched SPP height to integer values of ℓ for the chosen probe wavelength.²⁰ We stress that the appearance of a doughnut shaped intensity profile is only an approximation in the limit of small ratio w_0/R . Indeed, when $w_0/R \rightarrow 0$, the contribution of the second integral in Eq. (1) can be neglected and $J_{\ell \neq 0}(0)=0$ ensures a null on-axis (i.e., $\rho=0$) intensity.

In contrast, a complex intensity pattern is observed when w_0/R is large enough, as shown in Fig. 3 where $w_0/R=2$ and $\ell=1$. In that case the on-axis intensity is nonzero and the rotational symmetry is clearly broken. This can be explained as the result of interference between the field diffracted by the inner and the outer part of the illuminated SPP, which is described by the two integrals in Eq. (1), respectively. In

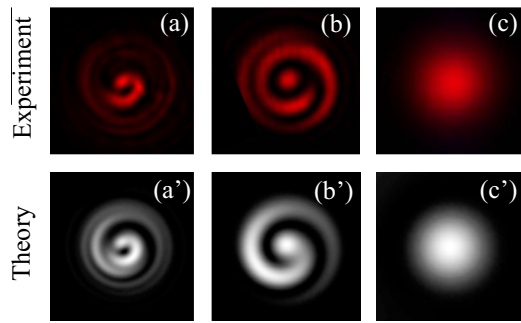


FIG. 3. (Color online) Diffraction intensity patterns at different observation planes for $w_0/R=2$ with $R=40\ \mu\text{m}$ and $\ell=1$. Upper row: experimental data. Bottom row: calculated profiles where the value of z is adjusted to visually match the observed pattern.

particular the far field pattern is now bell-shaped as shown in Figs. 3(c) and 3(c') that correspond to $\sim 10z_0$. Interestingly, the diffraction pattern exhibits a well-defined spiraling structure in the near field ($\lesssim z_0$), as illustrated in Figs. 3(b) and 3(b'). More generally a spiraling intensity pattern with ℓ -fold symmetry whose handedness depends on the sign of the topological charge (not shown here) can be found in the near field whatever is ℓ . Such a single beam interferometric scheme allows for the unambiguous characterization of the phase structure of any SPP with integer ℓ . This is illustrated in Fig. 4 for $\ell=(1,2,3,4)$. The observations are found to be in good agreement with simulations, which validate such an approach as a simple and efficient technique to characterize the spiraling complex transmittance of a SPP.

In conclusion, high fidelity direct laser polymerization of microscopic SPPs with integer topological charge has been realized. Both the structure of the micro-optical elements themselves and their use as vortex beam generators has been demonstrated. A simple, efficient, and reliable single beam

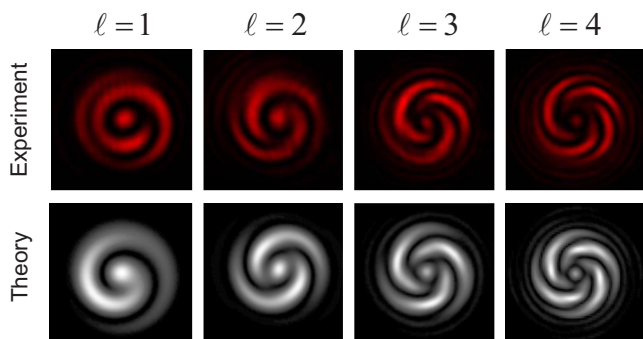


FIG. 4. (Color online) Spiraling diffraction intensity patterns in the observation planes where a well-defined ℓ -fold symmetry is visible. Here $w_0/R=2$ with $R=40\ \mu\text{m}$ and $\ell=(1,2,3,4)$. Upper row: experimental data. Bottom row: calculated profiles where the value of z is adjusted to visually match the observed pattern.

interferometric technique to characterize the helical wavefront of the obtained optical vortices has been proposed. The flexibility of the femtosecond-fabrication technique also enable us to demonstrate the ability to realize arrays of vortex generators or smart three-dimensional singular architecture at the micron scale. Moreover such a photopolymerization technique allows to envisage hybridization of vortex beam generator with additional functionalities, be they of a refractive (lenses, prisms, axicons) or a diffractive (gratings) nature toward versatile integrated devices.

S.J. is grateful for support by the Grant-in-Aid from the Ministry of Education, Science, Sports, and Culture of Japan (Grant No. 19360322). Part of the work was supported by EC's Seventh Framework Programme (LASERLAB-EUROPE, Grant No. 228334, OPTOBIO).

- ¹L. Li, R. R. Gattass, E. Gershgoren, H. Hwang, and J. T. Fourkas, *Science* **324**, 910 (2009).
- ²T. F. Scott, B. A. Kowalski, A. C. Sullivan, C. N. Bowman, and R. R. McLeod, *Science* **324**, 913 (2009).
- ³J. K. Gansel, M. Thiel, M. S. Rill, M. Decker, K. Bade, V. Saile, G. von Freymann, S. Linden, and M. Wegener, *Science* **325**, 1513 (2009).
- ⁴T. Baldacchini and R. Zadayan, *Opt. Express* **18**, 19219 (2010).
- ⁵J. Wang, R. C. Y. Auyeung, H. Kim, N. A. Charipar, and A. Piqué, *Adv. Mater. (Weinheim, Ger.)* **22**, 4462 (2010).
- ⁶M. Farsari and B. Chichkov, *Nat. Photonics* **3**, 450 (2009).
- ⁷M. Malinauskas, A. Žukauskas, V. Purlys, K. Belazaras, A. Momot, D. Paipulas, R. Gadonas, A. Piskarskas, H. Gilbergs, A. Gaidukevičiūtė, I. Sakellari, M. Farsari, and S. Juodkasis, *J. Opt.* **12**, 124010 (2010).
- ⁸D. Wu, S.-Z. Wu, L.-G. Niu, Q.-D. Chen, R. Wang, J.-F. Song, H.-H. Fang, and H.-B. Sun, *Appl. Phys. Lett.* **97**, 031109 (2010).
- ⁹L. Allen, M. W. Beijersbergen, R. J. C. Spreeuw, and J. P. Woerdman, *Phys. Rev. A* **45**, 8185 (1992).
- ¹⁰D. L. Andrews, *Structured Light and Its Applications: An Introduction to Phase-Structured Beams and Nanoscale Optical Forces* (Academic-Elsevier, Burlington, 2008).
- ¹¹S. N. Khonina, V. V. Kotlyar, M. V. Shinkaryev, V. A. Soifer, and G. V. Uspleniev, *J. Mod. Opt.* **39**, 1147 (1992).
- ¹²J. Courtial, K. Dholakia, D. A. Robertson, L. Allen, and M. J. Padgett, *Phys. Rev. Lett.* **80**, 3217 (1998).
- ¹³A. G. Peele, P. J. McMahon, D. Paterson, C. Q. Tran, A. P. Mancuso, K. A. Nugent, J. P. Hayes, E. Harvey, B. Lai, and I. McNulty, *Opt. Lett.* **27**, 1752 (2002).
- ¹⁴G. Knöner, S. Parkin, T. A. Nieminen, V. L. Y. Loke, N. R. Heckenberg, and H. Rubinsztein-Dunlop, *Opt. Express* **15**, 5521 (2007).
- ¹⁵A. Ovsianikov, J. Viertel, B. Chichkov, M. Oubaha, B. MacCraith, I. Sakellari, A. Giakoumaki, D. Gray, M. Vamvakaki, M. Farsari, and C. Fotakis, *ACS Nano* **2**, 2257 (2008).
- ¹⁶M. Malinauskas, A. Žukauskas, G. Bičkauskaitė, R. Gadonas, and S. Juodkasis, *Opt. Express* **18**, 10209 (2010).
- ¹⁷M. Malinauskas, G. Bičkauskaitė, M. Rutkauskas, D. Paipulas, V. Purlys, and R. Gadonas, *Lith. J. Phys.* **50**, 135 (2010).
- ¹⁸A. Ovsianikov, A. Gaidukevičiūtė, B. N. Chichkov, M. Oubaha, B. MacCraith, I. Sakellari, A. Giakoumaki, D. Gray, M. Vamvakaki, M. Farsari, and C. Fotakis, *Laser Chem.* **2008**, 1 (2008).
- ¹⁹M. J. Padgett and L. Allen, *Opt. Commun.* **121**, 36 (1995).
- ²⁰S. S. R. Oemrawsingh, J. A. W. van Houwelingen, E. R. Eliel, J. P. Woerdman, E. J. K. Versteegen, J. G. Kloosterboer, and G. W. 't Hooft, *Appl. Opt.* **43**, 688 (2004).